Proceedings of ICRC 2001: 1105 © Copernicus Gesellschaft 2001

ICRC 2001

Performance of the AMANDA-II Detector

R. Wischnewski[1] **for the AMANDA Collaboration**[2]

[1]DESY-Zeuthen, Platanenalle 6, D-15735 Zeuthen, Germany
[2]Complete author list is found at the end of this volume

Abstract. The AMANDA-II High Energy Neutrino Detector at the South Pole consists of 19 strings with 677 optical modules, and started operation February, 2000. We describe the detector design with the different technologies used for signal transmission. The larger geometry of the AMANDA-II detector, compared to the AMANDA-B10 detector operated in 1997, yields an improved sensitivity to high energy neutrinos, in particular a more uniform angular response. We present MC results on ν_μ and ν_e event rates and first results on separation of atmospheric ν_μ events.

1 Introduction

The AMANDA-II detector has been deployed in four South Pole campaigns between November 1995 and February 2000. The detector consists of optical modules (OM) arranged on vertical strings deployed to depths between 1300 m-2400 m. The main instrumented volume ranges from 1500 m-2000 m, and covers a cylinder of 200 m diameter (see fig.1).

A detailed analysis of data taken with the 10-string detector AMANDA-B10, commissioned in February 1997 and calibrated in 1998, resulted in the separation of the first large statistics sample of high energy neutrino events from an under-ice Cherenkov detector (Andres *et. al.*,2001), (Wiebusch *et al.*,2001). With specialized analysis techniques and a detailed modelling of the depth dependence of optical ice properties, this yielded 325 upgoing ν_μ events. The 4-string detector AMANDA-B4 had earlier been used to isolate a few vertical ν_μ events (Andres *et al.*,2000).

In this paper, we report first results of the AMANDA-II performance and give MC results for trigger level acceptance of high energy ν_μ and ν_e events. We discuss the improvement compared to the B10-detector in terms of atmospheric ν_μ event rate and angular acceptance.

Correspondence to: R. Wischnewski
(Ralf.Wischnewski@desy.de)

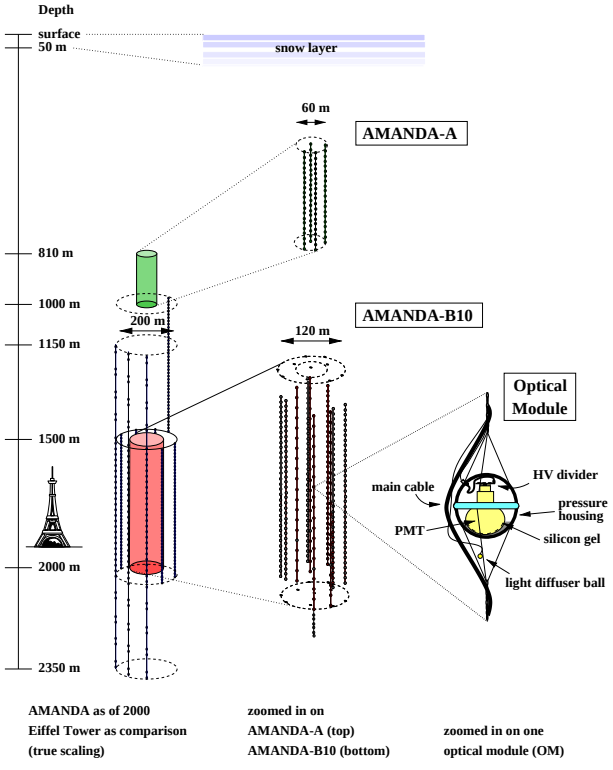

Fig. 1. The AMANDA-II detector, as of 2000.

2 The Detector

The deployment of AMANDA-II went along with a stepwise improvement of PMT signal transmission techniques. Strings 1-10 use passive OMs with electrical analog signal transmission, while strings 11-19 are based on analog fiber transmission (see table 1).

The first ten strings (deployed 1995/96 and 1996/97) form the inner AMANDA-II cylinder. Analog anode signals from the optical modules (OMs) are transmitted via electrical cable to the surface (coaxial for string 1-4, twisted pair for string 6-10). This cable also transmits the high voltage (see

fig.2).

Hamamatsu R5912-2 PMTs (8 inch) with 14 dynodes are operated at a gain of 10^9 in order to drive the one photoelectron-signal over 2 km cable. In spite of the strong dispersion along the cable, a time resolution of 5 nsec has been achieved.

The time offset t_o is calibrated by sending a laser-generated light pulse through an optical fiber from the surface to a diffuser ball close to the OM.

The large majority of the 375 OMs on strings 11-19, forming the outer ring of 200 m diameter, is based on analog fiber optic signal transmission without additional local electronics inside the OM.

The 123 OMs on strings 11-13 (1997/98) first used this new technique with optical fibers, both for calibration and for analog transmission of the PMT pulses (Karle *et al.*,1998). Electrical transmission was installed as backup. The fiber transmits the calibration signal to a diffuser ball inside the OM. An LED converts the PMT anode current into a light signal which is transmitted to the surface essentially without dispersion (see fig.2, middle). This results in high bandwidth, double pulse resolution of $\sim$20 nsec and does not need corrections for amplitude-dependent time slewing. The FWHM of pulses generated by a single photoelectron (p.e.) is 14 nsec (7 nsecs for OMs with active local electronics). Figure 3 shows a single photoelectron pulse as recorded with a twisted pair cable and with fiberoptic transmission. Drawback of the optical technique is a failure rate of about 10% during re-freezing of the ice, since optical connectors and fibers are more vulnerable to the high pressures.

For strings 14-19 (deployed in 1999/2000), the analog fiber OMs are operated at a gain of $\approx 3 \cdot 10^8$, allowing enhanced dynamic range (by using a transformer to multiply the PMT anode current that drives the LED transmitter).

All of the described OMs have in common that no active electronics has been deployed, and the high voltage for the PMT is provided directly from the surface. Two types of prototype active OM have been deployed. They are provided with low voltage and generate the HV locally using a Cockroft-Walton generator. Twenty three OMs are based on advanced analog fiber optic signal transmission (dAOM, see fig.2). A DC/DC converter in the OM converts the 60V-supply voltage to the low voltage required to operate a microprocessor and other integrated circuits. Thus one can operate the LED (13 OMs) or the Laser diodes (LD, on 10 OMs) with adjustable bias current, and amplify the anode signal in the OM, which allows for lower gain of the PMT and a higher dynamic range. Finally, another 41 OMs are built as digital optical modules (DOM), the prototype OM for the IceCube detector (Goldschmidt *et al.*,2001). In this approach the PMT waveforms are digitized in the OM and transmitted to the surface via an electrical cable. These OMs provide in addition fiber-optic analog signals, to allow for integration into the standard data aquisation system (DAQ).

The current DAQ reads out PMT amplitudes by using peak sensing ADC. The arrival times of pulses are recorded with Multi-Hit TDC, measuring the leading and falling edges of

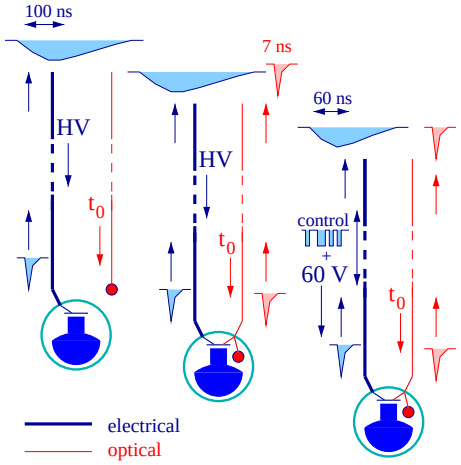

Fig. 2. Schematics of analog OM: electrical and fiber readout analog OM (AOM) and digitally controlled module (dAOM), from left to right. For digital OM (DOM), see (Goldschmidt *et al.*,2001).

up to 8 pulses. The time resolution is better than 5 nsecs. The dynamic range of the PMT is limited by a maximal anode current of about 15 p.e./10 nsec. The integrated dynamic range of the optical sensor can be much larger, since e.g. multiphoton pulses from distant muon tracks (or cascades) are dispersed in time due to scattering. For extremely high energy events an integrated dynamic range of more than 1000 photoelectrons is achievable.

In order to enhance the physics potential for high energy events, we plan to upgrade part of the DAQ with Flash ADC. This will allow to record more complex waveforms that are generated by muons and cascades of energies greater than $\approx 10TeV$. It is also planned to fully integrate the digitized waveforms that are recorded by the Digital Optical Modules on string 18.

3 Data and Response at Trigger Level

The AMANDA-II detector has been commissioned in February 2000, with a majority trigger condition of ≥ 24 OMs hit within a time intervall of 2.5 μs (since Feburary 2001, an additional trigger to record lower energy muons ($<$100 GeV) is in operation). With a data rate of $\sim$80kB/s, within $\sim$250 calendar days about 1.3 TB raw data are produced per season. At the South Pole, the data is written to magnetic tapes, and shipped out once per year. The high bandwidth TDRS satel-

Type	Technology	Number of OMs	Strings
AOM	Coax	80	1-4
AOM	Twisted pair	222	5-10
AOM	Fiber optic, LED, tw.p. backup	311	11-17,19
AOM	Fiber optic, LED/LD, local HV	23	14-19
DOM	Local HV (Fiber optic LED)	41	18

Table 1. AMANDA-II: Overview of analog (AOM) and digital (DOM) optical modules deployed.

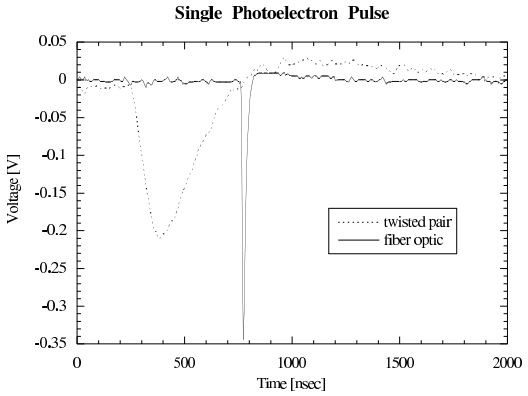

Fig. 3. Single photoelectron pulse recorded with twisted pair cable and optical fiber transmission.

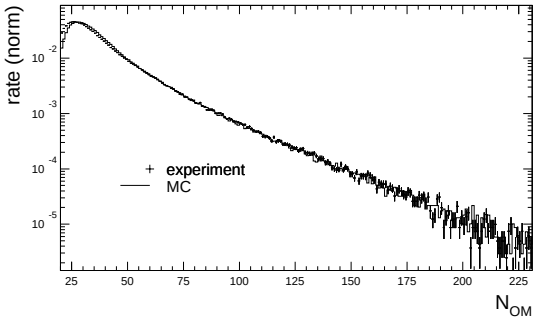

Fig. 4. Number of hit optical modules per event, N_{OM}, at trigger level (dots - experiment, histogram - MC prediction).

lite allowed to send out a substantial fraction of monitoring raw data to the northern hemisphere.

With the analysis of 2000 data recently started, we present first preliminary results. In figure 4, the normalized distribution of the number of hit optical modules per triggered event, N_{OM}, is shown, and compared to the Monte Carlo (MC) prediction from downgoing atmospheric muons (Desiati and Rhode *et al.*,2001). We find good agreement between MC and data up to highest observed multiplicites, indicating description of the main physics background for atmopsheric ν-search as well as for ultra-high energy analysis (Hundertmark *et al.*,2001).

In figure 5 we compare the $cos(\theta)$ and azimuth distributions for muon tracks reconstructed by the standard Likelihood method for downgoing muons. Again, MC and experiment agree reasonably well.

4 Signal expectation

The main goal of the AMANDA detector is the detection of astrophysical neutrino sources. Models of astrophysical neutrino sources, such as Active Galactic Nuclei (AGN), predict a harder neutrino spectrum than that of neutrinos generated within the atmosphere. This is illustrated in figure 6, where we show the expected spectrum of triggering atmospheric neutrinos (full line) as well as a spectrum of AGN neutrinos (dashed line, assuming equal flux of ν_μ and ν_e) with a hypothetical diffuse flux of $10^{-6} \cdot E^{-2}$ GeV sr^{-1} s^{-1}cm^{-2}. The thick lines correspond to charged current (CC) ν_μ reactions and the thin lines correspond to CC ν_e reactions. The number of events per year of effective livetime for the different channels triggered by Amanda-II are summarized in table 2. The

	Atmospheric	AGN
ν_μ	11000 (CC), 130 (NC)	853 (CC)
ν_e	162 (CC), 8.8 (NC)	103 (CC)

Table 2. Expected events per year triggering the AMANDA-II detector (as operated in the year 2000). Only events coming from the lower hemisphere were taken into account.

lower expectation of atmospheric CC ν_e events compared to that of CC ν_μ is an effect of the considerably lower flux and of the lower trigger volume. With the presently existing AMANDA detector, neutral current (NC) ν induced cascades are indistinguishable from CC ν_e induced cascades. Due to the low event rates in the cascade channel, detection of atmospheric neutrino induced cascades will be a challenge, see (Tabaoda and Kowalski *et al.*,2001). For the same reason, namely a lower background, this channel is promising when searching for astrophysical neutrinos.

5 Towards selection of atmospheric ν_μ

For a given detector, the reconstruction and the ν filter need to be adjusted to account for the present background, as well as the typical energy and angular spectrum of the expected signal. For the separation of atmospheric ν_μ events, as a performance proof of the detector and analysis techniques, we are guided by the procedures developed for the B10-detector (Wiebusch *et al.*,2001).

In a first analysis of 4 livetime days, we find good agreement between MC and data at trigger level, as well as at the first cut levels. Tuning of the final ν_μ-cuts to a low level physics and detector background is more delicate. With preliminary cuts, we have indication for a rate of about 4 atmospheric ν_μ's per livetime day.

We present in fig.7 a good candidate for an upward mov-

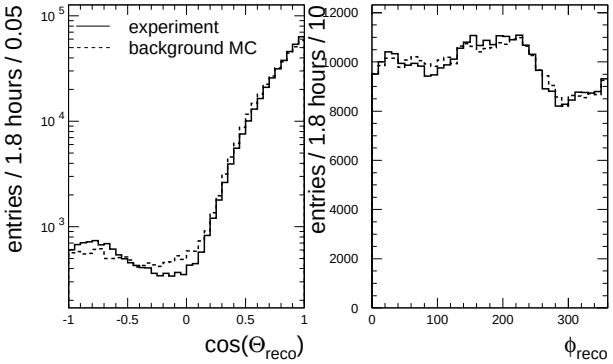

Fig. 5. Distribution of reconstructed zenith angle $cos(\Theta_{reco})$ (left) and azimuth angle Φ_{reco} (right, in degrees) at trigger level.

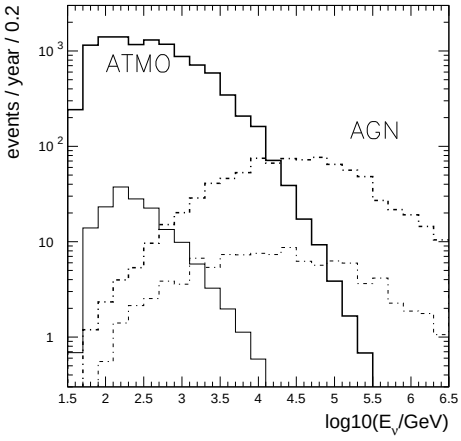

Fig. 6. Neutrino energy spectrum of events, triggering AMANDA-II. Shown are charged current ν_μ events (thick line) and charged current ν_e events (thin line) for atmospheric neutrinos (full line) and an AGN like spectrum (dashed line). Event rate is calculated per year of effective livetime.

ing muon, reconstructed close to the horizon (zenith angle = 105^o). This demonstrates sensitivity of AMANDA-II for the horizontal angular region.

In figure 8, the angular distribution for AMANDA-II is shown for the preliminary ν_μ-cuts. Comparison with the angular sensitivity for the B10-detector shows the gain in solid angle obtained by the larger detector (note that curves are normalized to same vertical upward rate). While the B10-detector was cutting most of the horizontal region we find an angular sensitivity up to 10^o below horizon.

6 Conclusion

The AMANDA-II detector with improved optical module technology is in stable operation. The detector yielded first promising results on atmospheric ν_μ-selection. Main improvements with respect to the AMANDA-B10 detector as operated in 1997 are the total atmospheric event rate, improved by at least a factor of two, an enlarged angular acceptance region and improved sensitivity for high energy events.

References

Andres, E., *et al.*, Astropatr. Phys. 13, 1, 2000.
Andres, E., *et al.*, Nature **410**, 441, 2001.
Desiati, P., Rhode, W. *et al.*, these proceedings.
Goldschmidt, A.,*et al.*, these proceedings.
Hundertmark, S. *et al.*, these proceedings.
Karle, A., *et al.*, Nucl. Inst. Meth. A 387 (1997) 274.
Tabaoda, I., Kowalski, M. *et al.*, these proceedings.
Wiebusch, Ch.,*et al.*, these proceedings.

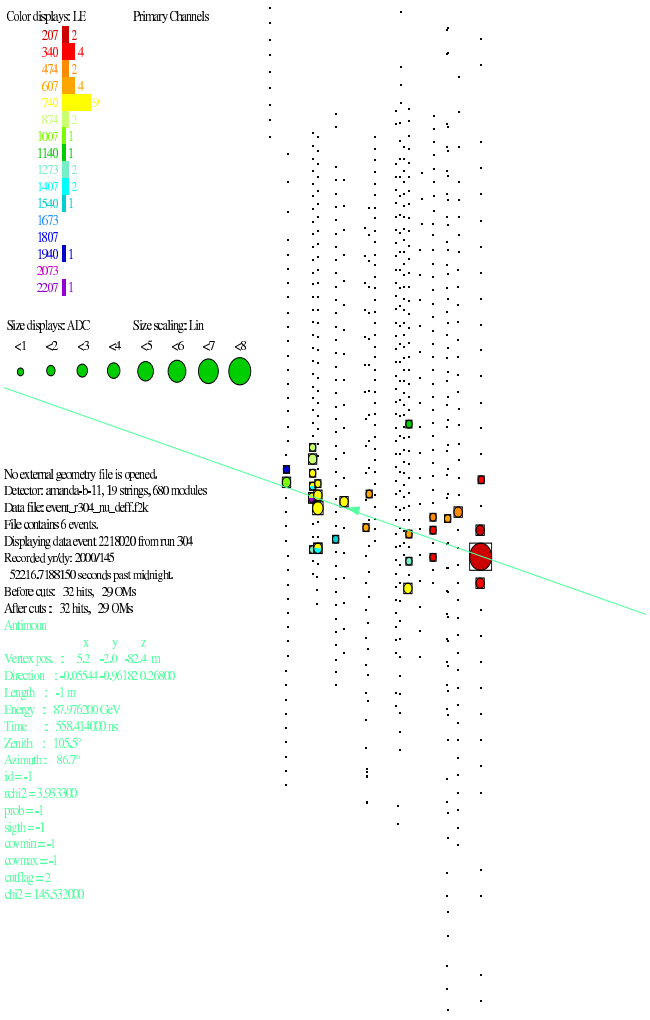

Fig. 7. An upward reconstructed AMANDA-II event close to the horizon.

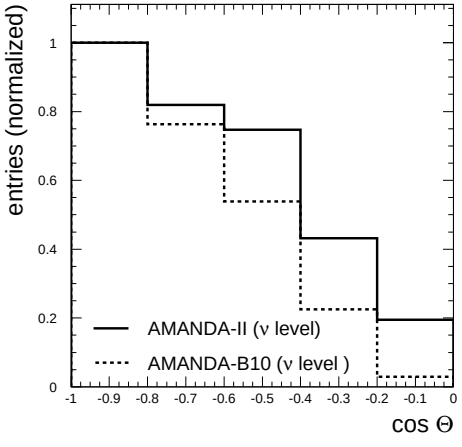

Fig. 8. Zenith angle distribution for atmospheric ν_μ MC events in AMANDA-II (full line, prel. cuts), compared to the AMANDA-B10 detector (dashed curve). Normalized for vertical tracks.